Mycobacterial virulence regulator integrates cAMP homeostasis with stress response and virulence

Hina Khan[1], Partha Paul[1, 2], Harsh Goar[1, 2], Ritesh Rajesh Sevalkar[1,3], Bhanwar Bamniya[1], Sangita Kachhap[1,4], Balvinder Singh[1] and Dibyendu Sarkar[1, *]

[1]CSIR-Institute of Microbial Technology, Sector 39 A, Chandigarh 160036, India

Running title: Mycobacterial cAMP homeostasis

Key Words: CRP-PhoP interaction; cAMP homeostasis; Mycobacterium; PhoP; virulence regulation

[2] Both contributed equally to this work

[3]Present address: Department of Microbiology, University of Alabama, Birmingham, Alabama, United States

[4]Present address: Jerzy Haber Institute of Catalysis and Surface Chemistry Polish Academy of Sciences, Niezapominajek 8, PL- 30239 Krakow, Poland

*Address correspondence to: Dibyendu Sarkar, CSIR-Institute of Microbial Technology, Tel.: 091-172-6665291; Fax: 091-172-2690585; E-mail: dibyendu@imtech.res.in

Abstract

Survival of *M. tuberculosis* within the host macrophages requires presence of the virulence regulator PhoP, but the underlying mechanism is yet to be understood. We discovered a signalling pathway which controls mycobacterial cAMP-inducible gene expression and cAMP homeostasis. We show that the level of intra-mycobacterial cAMP, one of the most widely used second messengers, is regulated by the virulence regulator PhoP, which recruits the cAMP responsive protein, CRP. We provide evidence to show that PhoP -dependent repression of cAMP specific phosphodiesterase Rv0805, which degrades cAMP hydrolytically, accounts for mycobacterial cAMP homeostasis. In keeping with these findings, genetic manipulation to inactivate PhoP-Rv0805-cAMP pathway leads to disruption of cAMP homeostasis, increased stress sensitivity and most critically, reduced mycobacterial survival in macrophages and animal models. Together, PhoP-dependent cAMP inducible gene expression and cAMP homeostasis represent a molecular checkpoint during intra-phagosomal survival and growth program of mycobacteria.

Introduction

M. tuberculosis, the causative agent of pulmonary tuberculosis, keeps encountering diverse stress conditions during infection, persistence and transmission of the disease (1, 2). However, the intracellular pathogen is exceptionally capable to adjust and survive within diverse intracellular environments. Mycobacterial adaptive response to different stages of infection is achieved via fine tuning of regulation of gene expression using an extensive repertoire of more than 100 transcriptional regulators, 11 two-component systems, 6-serine-threonine protein kinases and 13 alternative sigma factors suggesting that a very complex transcriptional program is important for *M. tuberculosis* pathogenesis. While regulation of gene expression as a consequence of interaction of tubercle bacilli with its immediate environment remains critically important (3), defining these regulatory pathways represent a major challenge in the field.

cAMP, one of the most widely used second messengers, impacts on a wide range of cellular responses in microbial pathogens including *M. tuberculosis* (4). A large number of genome-encoded adenylate cyclases in *M. tuberculosis* complex is remarkable in view of a single adenylate cyclase of most bacteria and fungi (5, 6). More importantly, at least 10 of the 17 enzymes show biochemical activity, and one of these (Rv0386) is required for virulence (7). Consistent with the abundance of adenylate cyclases, mycobacteria produce high levels of cAMP relative to other bacterial species (8). Importantly, cAMP levels are elevated upon infection of macrophages by pathogenic mycobacterium (8, 9) and addition of cAMP to growing cultures of *M. tuberculosis* significantly impacts mycobacterial gene expression (10). Agarwal and colleagues have shown that bacterial cAMP burst, upon infection of macrophages, improves bacterial survival by interfering with host signalling pathways (7).

Previous *in silico* analyses had identified two out of 10 predicted nucleotide binding proteins of *M. tuberculosis* as members of the CRP/FNR superfamily of transcriptional regulators. These are CRP, encoded by Rv3676 and CMR, encoded by Rv1675c, respectively. Off these two, CRP become activated upon cAMP binding, and functions as a global regulator of ~ 100 genes (11-13), and deletion of the *crp* locus significantly impairs mycobacterial growth and attenuates virulence of the

bacilli in a mouse model (13). In contrast, CMR (cAMP macrophage regulator) is necessary for regulated expression of genes like *mdh*, *groEL2* and *Rv1265* in response to variations of cAMP level during macrophage infection, and *Δcmri*-H37Rv grows comparably well within macrophages as that of the WT-H37Rv (14). However, very little is known about the mechanism underlying mycobacterial cAMP homeostasis, and regulation of cAMP- dependent mycobacterial gene expression.

To identify mechanism of cAMP homeostasis, we hypothesized that the level of cAMP could be determined by the *phoP* locus linking numerous diverse stress conditions, which signal activation of adenylate cyclases that synthesize cAMP (15). Interestingly, our results connect response regulator PhoP with intra-mycobacterial cAMP level. To investigate how PhoP contributes to regulation of mycobacterial cAMP level, we discovered that the virulence regulator controls expression of cAMP-specific phosphodiesterase Rv0805, which hydrolytically degrades cAMP. This observation accounts for a consistently lower level of cAMP in a *ΔphoP*-H37Rv relative to the WT bacilli, and establish the molecular mechanism of cAMP homeostasis, absence of which strongly impacts phagosome maturation, and reduces mycobacterial survival within macrophages and animal models. Global expression profiling uncovers that PhoP-depletion or Rv0805-over expression significantly influences numerous mycobacterial genes which belong to CRP regulon. We next identify protein -protein contacts between PhoP and CRP as a novel mechanism to control regulatory network of cAMP-dependent gene expression. Together, PhoP-dependent cAMP inducible gene expression and cAMP homeostasis represent a molecular checkpoint during intra-phagosomal survival and growth program of mycobacteria.

RESULTS

Intra-mycobacterial cAMP level is regulated by the *phoP* locus

M. tuberculosis encounters a hostile environment within the host. In order to survive in an intracellular environment, it must respond appropriately. Among the hostile conditions is the acidic pH stress and exposure to host immune effectors such as NO (16-18). A growing body of evidence

connects mycobacterial *phoP* locus with multiple stress conditions, including acid stress (19-21), heat-shock (22, 23) and integration of acid stress response to redox homeostasis (24). As stress conditions are often linked to variation of cAMP levels, we compared cAMP levels of WT-H37Rv and Δ*phoP*-H37Rv mutant, grown under normal as well as specific stress conditions, like NO stress and acid stress (see Methods) (Fig. 1A). Interestingly, *ΔphoP*-H37Rv showed a significantly lower level of cAMP relative to the WT bacilli, both under normal and stress conditions. More importantly, complementation of the mutant could restore cAMP to the WT level. Because bacterial growth often varies under stress conditions, and growth inhibition can influence cAMP level, we compared survival of the mycobacterial strains under normal and indicated stress conditions by determining their CFU values (Fig. S1A). Our results suggest that despite exposure to indicated stress conditions, both the WT- and *ΔphoP*-H37Rv display comparable growth, indicating that growth inhibition of the mutant under defined stress conditions do not account for lower cAMP level. From these results, we conclude that PhoP plays a major role in maintaining intra-mycobacterial cAMP level.

To investigate the possibility that *ΔphoP*-H37Rv secretes out more cAMP and therefore, shows a lower cytoplasmic level, we compared cAMP secretion of WT and the mutant (Fig. 1B). We show that the mutant reproducibly secretes lower amount of cAMP relative to the WT bacilli, and cAMP secretion is fully restored in the complemented *ΔphoP*-H37Rv mutant. As the fold difference of secretion (~ 3- fold) is not much different relative to the fold difference in intra-mycobacterial cAMP level (2±0.4- fold), we conclude that most likely lower cAMP level of the mutant is not due to its higher efficacy of cAMP secretion. Fig. S1B confirms absence of autolysis of mycobacterial cells as GroEL2 was undetectable in the culture filtrates (CF).

We next investigated role of the *phoP* locus on expression of mycobacterial adenylate cyclases and PDE, which synthesizes and degrades cAMP, respectively (Fig. 1C). Our RT-qPCR results show that *phoP* does not regulate expression of adenylate cyclases including Rv0386, Rv1264, Rv1647 and Rv2488c (7, 15, 25, 26). However, *phoP* shows a significant activation of Rv0891c

(4±0.05-fold), and repression of Rv0805 (6.5±0.7-fold) expression, respectively (Fig. 1C). Expression of Rv0805, but not Rv0891c was restored in a *ΔphoP*-H37Rv complemented strain. Although Rv0891c has been suggested as one of the *M. tuberculosis* H37Rv adenylate cyclases, the protein lacks most of the important residues conserved for adenylate cyclase family of proteins (27). Conversely, Rv0805 encodes for a cAMP-specific phosphodiesterase (PDE), present only in slow growing pathogenic *M. tuberculosis* (28-30). Therefore, we focussed our attention on the biological significance of regulation of Rv0805 PDE expression by PhoP. Importantly, expressions of Rv1357c and Rv2837c, encoding PDEs for cyclic di-GMP and cyclic di-AMP, respectively, remained unaffected in Δ*phoP*-H37Rv. From these results, we surmise that *M. tuberculosis* PhoP functions as a repressor of cAMP specific PDE Rv0805.

With the results showing PhoP-dependent regulation of Rv0805 expression, we wished to examine whether PhoP binds to Rv0805 promoter. An EMSA experiment suggests that P~PhoP appears to bind to end-labelled Rv0805 promoter region (spanning -150 to +51 of the upstream Rv0805 regulatory region relative to the ORF start site) with a relatively lower affinity (Fig. S1C). In keeping with this, a closer inspection of the promoter for a possible PhoP binding site using ChIP-seq derived PhoP consensus sequence (31) reveals presence of a likely binding sequence (CGACCCCGCGATCACAGT) spanning -110 to -127 (relative to the ORF start site) of the regulatory region of Rv0805. Clearly, more studies will be required to fully understand the mechanism of PhoP-dependent Rv0805 repression.

PhoP contributes to mycobacterial stress response by maintenance of cAMP homeostasis

To examine the effect of Rv0805 on mycobacterial cAMP level, we used a recombinant *M. tuberculosis* H37Rv expressing a copy of *Rv0805* (referred to as H37Rv-Rv0805) (Fig. 2A). To this end, *M. tuberculosis* Rv0805 ORF was cloned within the multicloning site of pSTki (32) between the EcoRV and HindIII sites under the control of P_{myc1}*tetO* promoter. Ectopic expression of Rv0805, as

verified by the mRNA level (Fig. S2A), does not influence mycobacterial growth under normal conditions (Fig. S2B). We next assessed the impact of Rv0805 on intra-mycobacterial cAMP. Consistent with a previous study (7), H37Rv-Rv0805 showed a significantly lower (2.1± 0.7-fold) level of intra-mycobacterial cAMP relative to WT-H37Rv (Fig. 2A). To confirm that lowering of mycobacterial cAMP is attributable to Rv0805 expression, we expressed Rv0805^{M}, a mutant Rv0805 lacking phosphodiesterase activity, in WT-H37Rv. The mutant Rv0805^{M} was constructed by changing a conserved Asn-97 to Ala as structural data coupled with biochemical evidences reveal that Asn-97 within the enzyme active site plays a key role in phosphodiesterase activity (28, 29). WT-H37Rv ectopically expressing Rv0805 or Rv0805^{M} (referred to as H37Rv-Rv0805, and H37Rv-0805^{M}, respectively) as verified by the corresponding mRNA levels (Fig. S2A), did not influence bacterial growth under normal conditions (Fig. S2B). However, H37Rv-0805^{M} showed an almost comparable cAMP level as that of WT-H37Rv (Fig. 2A), suggesting that lower intra-mycobacterial cAMP level of H37Rv-Rv0805 (similar to that of *ΔphoP*-H37Rv) is indeed attributable to phosphodiesterase activity of Rv0805. These observations are in agreement with a previous report describing influence of expressing Rv0805 on mycobacterial cAMP level (7). Notably, cAMP level of H37Rv-Rv0805 was comparable to that of *ΔphoP*-H37Rv. These results are consistent with a model suggesting that PhoP-dependent repression of Rv0805 accounts for a significantly lower level of cAMP in Δ*phoP*-H37Rv relative to WT-H37Rv.

To examine whether cAMP level influences mycobacterial susceptibility to stress, we compared *in vitro* mycobacterial growth under acidic pH (pH 4.5) (Fig. 2B). As observed previously, *ΔphoP*-H37Rv showed a significant growth inhibition relative to WT-H37Rv under low pH (pH 4.5) (20). Importantly, H37Rv-Rv0805 (but not H37Rv-Rv0805^{M}) displayed a comparable susceptibility to acidic pH as that of *ΔphoP*-H37Rv. However, all four mycobacterial strains grew comparably well under pH 7.0. Next, to compare growth of H37Rv-Rv0805 and WT-H37Rv under oxidative stress, cells were grown in presence of increasing concentrations of diamide, and examined by microplate-based Alamar Blue assays (Fig. 2C). We observed that similar to *ΔphoP*-H37Rv, H37Rv-Rv0805 (but

not H37Rv-Rv0805^{M}) was significantly more susceptible to diamide stress as compared to WT-H37Rv (Fig. 2D). To verify sensitivity of the mycobacterial strains to Cumene Hydrogen Peroxide (CHP), we next grew mycobacterial strains in presence of 50 µM CHP for 24 hours and determined their survival by enumerating the CFU values (Fig. 2E). Because of the bactericidal property of CHP, we were unable to perform Alamar Blue-based survival assays requiring a longer time. Our CFU data on survival assays highlight that in the presence of CHP, H37Rv-Rv0805 (but not H37Rv-Rv0805^{M}) displayed a significantly higher growth inhibition relative to WT-H37Rv. Importantly, this was also the case for *ΔphoP*-H37Rv (33), that displayed a comparable stress sensitivity as that of H37Rv-Rv0805. Together, these results demonstrate a comparably higher susceptibility of *ΔphoP*-H37Rv, and H37Rv-Rv0805 to acidic pH and oxidative stress relative to WT-H37Rv and establish a link between cAMP homeostasis to mycobacterial stress response, suggesting that at least one of the mechanisms by which PhoP contributes to global stress response is by maintenance of mycobacterial cAMP homeostasis.

The results showing a significantly higher stress-sensitivity of H37Rv-Rv0805 relative to WT-H37Rv, prompted us to investigate whether altered cell wall structure/properties of H37Rv-Rv0805 contributes to elevated stress sensitivity. In fact, using *M. smegmatis* as a host strain, Rv0805 over-expression has been suggested to influence cell wall permeability (30). Thus, we compared (i) colony morphology of the relevant strains and (ii) expression level of lipid biosynthetic genes, which are known to impact cell wall structure of the bacilli (34). Our results demonstrate that in striking contrast to *ΔphoP*-H37Rv, both H37Rv-Rv0805 or H37Rv-Rv0805^{M} display a largely similar colony morphology as that of the WT-H37Rv (Fig. S2C) with comparable expression of complex lipid biosynthesis genes (Fig. S2D). Although we cannot rule out the possibility of any other factor(s) influencing cell wall properties, together these results facilitate an integrated view of our results suggesting that higher susceptibility of H37Rv-Rv0805 to stress conditions, is most likely controlled by mycobacterial cAMP level.

cAMP level and its effect on mycobacterial pathogenicity

To investigate the effect of mycobacterial cAMP level on pathogenesis, we next studied infection of murine macrophages by WT-H37Rv, H37Rv-Rv0805, and H37Rv-Rv0805^{M} (Fig. 3A). Consistent with previous studies (35, 36), WT-H37Rv inhibited phagosome maturation. However, infection of macrophages with H37Rv-Rv0805 and *ΔphoP*-H37Rv matured into phagolysosomes, suggesting increased trafficking of the bacilli to lysosomes. Interestingly, under identical conditions H37Rv-Rv0805^{M} could effectively inhibit phagosome maturation just as the wild-type bacilli. Results from the co-localization experiments are plotted in Fig. 3B and as Pearson's correlation co-efficient of the quantified co-localization signals in Fig. 3C. Thus, from bacterial co-localization data showing reduced ability of H37Rv-Rv0805 (but not H37Rv-Rv0805^{M}) to inhibit phagosome maturation, we conclude that ectopic expression of Rv0805 impacts phagosome maturation via PhoP-dependent cAMP homeostasis. These results argue in favour of a role of PhoP in blocking phagosome-lysosome fusion in macrophages by maintenance of mycobacterial cAMP homeostasis.

To examine the effect *in vivo*, mice were infected with mycobacterial strains via the aerosol route. Day 1 post-infection, CFU analyses revealed that a comparable count of four mycobacterial strains (~100 bacilli) were present in the mice lungs. However, for H37Rv-Rv0805, the CFU recovered from infected lungs 4 weeks post- infection declined by ≈218-fold relative to the lungs infected with WT-H37Rv (Fig. 3D). In contrast, for H37Rv-Rv0805^{M}, the CFU recovered from infected lungs after 4 weeks of infection marginally declined by ≈7-fold relative to the lungs infected with WT-H37Rv. These results suggest a significantly compromised ability of H37Rv-Rv0805 to replicate in the mice lungs. Note that *ΔphoP*-H37Rv, under the conditions examined, showed a ≈246-fold lower lung burden compared to WT-H37Rv. In keeping with these results, while the WT-H37Rv disseminated to the spleens of infected mice, a significantly lower count of H37Rv-Rv0805 was recovered from the spleens after 4 weeks of infection (Fig. 3E). Thus, we conclude that one of the reasons which accounts for an attenuated phenotype of *ΔphoP*-H37Rv in both cellular and animal models is attributable to

PhoP-dependent repression of phosphodiesterase activity of Rv0805, which controls mycobacterial cAMP homeostasis.

M. tuberculosis H37Rv is known to persist within granulomas where it is protected from the anti-mycobacterial immune effectors of the host. Histopathological evaluations showed that WT-H37Rv-infected lung sections displayed aggregation of granulocytes within alveolar spaces which degenerate progressively to necrotic cellular debris. In contrast, *ΔphoP*-H37Rv and H37Rv-Rv0805 showed less severe pathology as indicated by decreased tissue consolidation, smaller granulomas, and open alveolar space (Fig. 3F). These results suggest that ectopic expression of Rv0805 in WT-H37Rv is functionally equivalent to depletion of PhoP, suggesting that failure to maintain cAMP homeostasis accounts for attenuated phenotype of the bacilli and an absence of immunopathology in the lungs of infected mice.

PhoP-dependent Rv0805 expression impacts mycobacterial CRP regulon

We next undertook a global transcriptional profiling to compare genes that are differentially expressed in Δ*phoP*-H37Rv and H37Rv-Rv0805. Thus, both mycobacterial strains were grown in 7H9 medium, total RNA was isolated and subjected to RNA sequencing [Tables S1, and S2, respectively (Excel spreadsheet)]. Our results show that ectopic expression of Rv0805 significantly impacts mycobacterial transcriptome. Over-expression of Rv0805 leads to activation of 270 genes (>1.5 fold; $p < 0.05$) and down-regulation of 94 genes (>1.5 fold; $p < 0.05$). Interestingly, a significant overlap was observed between genes regulated by over-expression of Rv0805 and those regulated by PhoP (Fig. S3). Figs. S3A and S3B represent heat-maps comparing data from *ΔphoP*-H37Rv and H37Rv-Rv0805 relative to WT-H37Rv, respectively, displaying differential expression of 28 (21 upregulated and 7 down regulated) overlapping genes. These include genes involved in the metabolic pathways, virulence and detoxifications, cell wall biosynthesis, information pathways, PE/PPE proteins, and lipid metabolism. Notably, genes which are upregulated in the PhoP-depleted mutant are also activated in H37Rv-Rv0805. Likewise, genes which were down-regulated in *ΔphoP*-H37Rv, also

showed lower expression in H37Rv-Rv0805 (compare Fig. S3C and Fig. S3D). These transcriptomic data are consistent with PhoP functioning as a repressor of Rv0805 (see also Fig. 1C), suggesting that PhoP-depletion largely mimics Rv0805 over-expression. Figs. S3C and S3D compare Venn diagram showing activation and repression of gene expression in *ΔphoP*-H37Rv, and H37Rv-Rv0805, respectively relative to WT-H37Rv [Tables S3, and S4, respectively (Excel spreadsheet)]. These results establish that PhoP-regulated Rv0805 expression, functions by targeting cAMP-inducible mycobacterial genes. Remarkably, we discovered that 15 out of 28 common genes, impacted either by PhoP depletion or Rv0805 over-expression, belong to the CRP regulon (37). Table 1 summarizes upstream regulatory region of these commonly regulated genes comprising indicated binding sites of both PhoP and CRP.

We next compared relative expression of representative CRP regulon genes in WT-, *ΔphoP*-H37Rv, and H37Rv-Rv0805, under normal and indicated stress conditions (Fig. 4A). Consistent with the transcriptomic data, RT-qPCR experiments demonstrate that the above cAMP- inducible genes are regulated by both PhoP and Rv0805. We observed while PhoP functions as an activator of CRP-regulated genes, Rv0805 acts as a repressor of these genes. These results integrate PhoP-controlled Rv0805 expression contributing to cAMP homeostasis and PhoP-dependent cAMP-inducible gene expression. Since we noted elevated expression of cAMP-inducible genes in the complemented mutant, we compared *phoP* expression in WT-H37Rv and complemented *ΔphoP*-H37Rv (Fig. S4). Our results demonstrate that *phoP* expression level is reproducibly higher in the complemented mutant (relative to the WT bacilli) both under normal conditions as well as during growth under low pH conditions. These results possibly account for an elevated mRNA levels of a few representative genes in the complemented mutant relative to WT-H37Rv (Fig. 4A). However, relatively poor restoration of gene expression in the complemented mutant under acid stress is possibly related to inadequate activation of PhoPR under acidic pH. We speculate that activation of PhoPR under low pH is somewhat compromised in the complemented mutant.

To examine whether PhoP regulates *crp*, expression levels of *crp* in WT-, and *ΔphoP*-H37Rv was compared (Fig. 4B). The results clearly show that *crp* is not under the regulation of *phoP* locus. As a positive control, low pH-inducible *aprA* which belongs to the PhoP regulon, showed a significantly altered expression when compared between WT- and *ΔphoP*-H37Rv. These results suggest that PhoP-dependent regulation of cAMP-inducible genes is not attributable to PhoP controlling CRP expression. Next, to investigate whether PhoP is recruited within the promoters of cAMP -inducible genes, Flag-tagged PhoP was ectopically expressed in WT-H37Rv using mycobacterial expression vector p19Kpro (38), and ChIP-qPCR was carried out using anti-Flag antibody as described in the Experimental procedures. We found that relative to mock (no antibody control) sample, PhoP is significantly enriched at the *whiB1*, *icl1* and *umaA* promoters by 12.4±0.4, 4.4±0.5, and 6.2±0.9-fold, respectively (Fig. 4C). As controls, *gapdh*-specific qPCR did not show any enrichment, whereas *espA*, a target promoter of PhoP(39), showed 6.0±0.3 -fold enrichment relative to the mock sample, further confirming specific recruitment of PhoP within the cAMP-inducible promoters. These results are consistent with the presence of PhoP binding site within these cAMP-inducible mycobacterial promoters (Table 1).

PhoP interacts with CRP

Having identified proximal binding sites of PhoP and CRP within numerous promoters of CRP regulon, we sought to investigate whether these two regulators interact to each other. During *in vitro* pull-down assays, recombinant PhoP was expressed as a GST fusion protein, and immobilized on glutathione-Sepharose; following incubation with crude lysate of *E. coli* cells expressing His_6-tagged CRP, the column-bound proteins were eluted by 20 mM reduced glutathione. Importantly, we could detect presence of both the proteins in the same eluent fraction by immuno-blot analysis (lane 1, Fig. 5A). However, we were unable to detect CRP with only GST- tag (lane 2) or the resin alone (lane 3), allowing us to conclude that PhoP interacts with CRP.

We further investigated PhoP-CRP interaction using mycobacterial protein fragment complementation (M-PFC) assay (Fig. 5B) (40). Thus, we generated a bait and prey plasmid pair as C-terminal fusions with complementary fragments of mDHFR. PhoP was expressed from integrative plasmid pUAB400 (see Tables S5 and S6 for lists of oligonucleotide primer sequences and plasmids, respectively). Likewise, *crp* and *phoR* encoding ORFs were expressed from the episomal plasmid pUAB300. The corresponding plasmids were co-transformed in *M. smegmatis* and transformants were selected on 7H10/kan/hyg plates. Interestingly, cells co-expressing PhoP and CRP grew well in presence of TRIM (Fig. 5B). In contrast, *M. smegmatis* harbouring empty vector controls showed no detectable growth on 7H10/TRIM plates while all these strains grew well on 7H10 plates lacking TRIM. However, under identical conditions, *M. smegmatis* co-expressing PhoP and CMR did not show any detectable growth (Fig. 5C). To examine the possibility whether variable expression of *M. tuberculosis cmr* and *crp* in *M. smegmatis* contributes to the interaction data, we compared expression levels of the regulators by RT-qPCR (Fig. 5D). Our results suggest that the two regulators CRP and CMR are expressed in *M. smegmatis* at a comparable level, suggesting that altered expression of CMR most likely does not account for lack of growth of the bacteria. Thus, M-PFC data unambiguously suggest specific interaction between PhoP-CRP.

To examine the influence of phosphorylation of PhoP, next we performed M-PFC experiment using phosphorylation-defective PhoPD71N and CRP (Fig. 5E). We found that PhoPD71N is unable to interact with CRP, underscoring the importance of phosphorylation of PhoP on PhoP-CRP interaction. To examine the interaction *in vivo*, whole cell lysate of *ΔphoP*-H37Rv expressing His-tagged PhoP was incubated with Ni-NTA as described previously (39). As expected, both CRP and PhoP were detected in the crude lysate (lane 1, Fig. 5F). More importantly, upon elution of bound proteins, the eluent showed a clear presence of CRP (lane 3), suggesting specific *in vivo* interaction between PhoP and CRP. As a control, we were unable to detect CRP from the eluent using cell lysates of Δ*phoP*-H37Rv carrying empty vector (p19Kpro) alone (lane 2).

To probe structural arrangement of the interacting regulators, X-ray diffracted structures of PhoP (PBDID: 3ROJ) and a dimer of CRP were docked employing ZDOCK (41) (Figs. S5A-D). *M. tuberculosis* CRP structure is available both in free- (PDB ID: 3D0S) and cAMP-bound form (PDB ID: 4A2U). Although these structures are nearly identical (RMSD less than 0.1A° for backbone atoms), cAMP induces a conformational change in the C-terminal DNA binding domain (42). Therefore, PhoP-CRP rigid-body-docking utilized structural coordinates of both free (Fig. S5A-B) and cAMP-bound CRP (Fig. S5C-D). The missing amino acid residues of PhoP structure (142-147) were modeled using MODELLER (43, 44), the docked complexes were ranked using ZRANK (45), and top-ranked complexes were identified using PDBePISA webserver (46). Next, nearly two thousand top scoring complexes were screened, and further re-ranked using a scoring function to yield six docked complexes. Two possible models of interaction emerged based on the above analyses. The first one of the two (based on free CRP) suggests interaction between the dimerization domain of PhoP with CRP (Fig. S5A), whereas the second model predicts that the C-domain of PhoP contacts CRP (Fig. S5B). Conversely, using cAMP-bound CRP as the structural template, ZDOCK predicted two possible interaction models. While first one of the two suggests involvement of the N-domain of PhoP (Fig. S5C), the other model is indicative of involvement of the PhoP linker in contacting CRP (Fig. S5D). In summary, docking analysis suggests that it is the N-terminal domain of CRP, which appears to interact with PhoP. In contrast, away from the interaction interface, the C-terminal domain remains available to interact with DNA, arguing in favour of the fact that absence of cAMP is unlikely to influence interaction interface of CRP. These results justify absence of cAMP in experiments investigating PhoP-CRP interaction.

To examine between the two possibilities, we assessed role of different stretches of PhoPN in PhoP-CRP interactions (Fig. S5E). *In vitro* pull-down assays using mutant GST-PhoP proteins (each with three potential CRP- contacting residues of PhoP replaced with Ala) with His-tagged CRP displayed effective protein-protein interaction as that of the WT PhoP (compare lane 1 and lanes 2-6). These results suggest that either PhoPN does not contribute to PhoP-CRP interactions or possibly a

constellation of residues, but not a few residues of PhoPN, in a single stretch is involved in PhoP-CRP interaction(s). Next, pull down assays using His-tagged CRP and a linker deletion mutant of PhoP [PhoPLAla5, replacing 5 residues spanning Gly^{142} to Pro^{146} with Ala, which remains functional (47)], suggest that PhoP linker does not appear to contribute to PhoP-CRP interaction(s) (compare lane 1 and lane 2, Fig. S5F). Although PhoP-CRP interaction studies were performed in the absence of cAMP, we next investigated whether cAMP binding to CRP is required for PhoP-CRP interaction. Thus, we performed *in vitro* interaction studies using CRP mutants (CRPG79A, and CRPT90A), deficient for cAMP binding (Fig. S5G). The mutations were designed based on previously-reported CRP structure defining the cAMP binding pocket of the regulator (48). Our pull-down assays demonstrate that the mutant CRP proteins interact with PhoP as effectively as that of the wild-type CRP, allowing us to conclude that cAMP binding to CRP is not required for PhoP-CRP interaction. It is noteworthy that over a range of protein concentrations, both the mutant proteins showed effective DNA binding to end-labelled whiB1up with a comparable affinity as that of the WT-CRP (Fig. S5H). Thus, we conclude that the mutant proteins most likely retain native structure and/or fold as that of WT-CRP. These results are in keeping with cAMP-independent functioning of *M. tuberculosis* CRP (37, 49-51).

PhoP promotes CRP recruitment and regulates cAMP-inducible gene expression

We next probed PhoP-CRP interaction using His-tagged full-length CRP and PhoP domains as GST-fusion constructs (Fig. 6A). PhoPN and PhoPC were previously shown to be functional on their own for phosphorylation and DNA binding activity, respectively (47). Importantly, PhoPN (comprising residues 1-141) showed effective protein-protein interaction with CRP (lane 1). However, PhoPC (comprising residues 141-247), under identical conditions, did not display an effective interaction with CRP (lane 2). To identify the corresponding interacting domain of CRP, we next used GST-PhoP and His-tagged CRP-domain constructs (Fig. 6B). Interestingly, N-terminal domain of CRP, CRPN (comprising residues 28-116) co-eluted with GST-PhoP (lane 1); however, CRPC (comprising residues 146-224) under identical conditions, did not co-elute with GST-PhoP (lane 2), suggesting

specific interaction between CRPN and PhoP. Together, we surmise that PhoP-CRP interaction is mediated by the N-domains of the corresponding regulators. These results are in agreement with rigid body docking study using PhoP and CRP structures (Fig. S5A-D).

To examine how a representative promoter DNA accommodates both the regulators *in vitro*, we performed an EMSA experiment using end-labelled whiB1up1 and purified regulators PhoP and CRP (Fig. 6C). Note that upstream regulatory region of *whiB1* showed the most efficient *in vivo* recruitment of PhoP in ChIP assay (Fig. 4C). Consistently, P~PhoP showed ≈20- fold more efficient DNA binding to whiB1up (326- bp fragment spanning -266 to +60 relative to the whiB1 ORF start site) compared to the unphosphorylated regulator (compare lanes 2-4 and lanes 5-7 [based on limits of detection in these assays]; Fig. S6A). Additional experiments to identify the core binding site of PhoP using PCR-amplified overlapping promoter fragments show that although 111-bp whiB1up1 (-266 to -156 with respect to the ORF start site of whiB1) efficiently binds to P~PhoP (lanes 2-3), two other fragments whiB1up2 (-156 to -46), and whiB1up3 (-50 to +60) failed to form a stable complex with P~PhoP (lanes 5-6, and lanes 8-9, respectively), indicating absence of PhoP binding site downstream of -156 nucleotide of the whiB1 promoter (Fig. S6B). Next, in EMSA experiments, presence of 10- and 20-fold molar excess of unlabelled whiB1up1 efficiently competed out PhoP binding (lanes 3-4, Fig. S6C). However, an identical fold excess of unlabelled whiB1up3 resulted in a minor variation of PhoP binding (<5% effect on DNA binding; lanes 5-6) to whiB1up1 compared to 'no competitor' control (lane 2), reflecting that PhoP binding to whiB1up1 is sequence-specific. This result is consistent with the presence of two neighbouring PhoP boxes (31, 52) comprising a 7-bp direct repeat motif spanning nucleotides -97 to -91, and -86 to -80 relative to the *whiB1* transcription start site (Table 1). To verify the importance of this motif, mutations were introduced within both the repeat units of whiB1up1 as shown in the figure (Fig. S6D). A labelled DNA fragment carrying only these changes (whiB1up1mut) failed to form a stable PhoP - promoter DNA complex, while the WT promoter (whiB1up1) under identical conditions, exhibited efficient DNA binding (compare lanes 2-4

with lanes 6-8, Fig. S6E). These results suggest that PhoP most likely binds to whiB1up1 by sequence-specific recognition of the 7-bp direct repeat motif.

To examine the importance of PhoP binding site in transcription regulation, whiB1upmut was cloned into pSM128, a promoter-less mycobacterial reporter plasmid (53) and used as a transcription fusion in *M. smegmatis*. The strain harbouring transcriptional fusions were co-transformed with pME1mL1-*phoP* (54), and grown in 7H9 medium in absence or presence of 50 ng/ml ATc, an inducer of PhoP expression, as described previously (34). Consistent with *phoP*-dependent *in vivo* activation of *whiB1* (Fig. 4A), with induction of PhoP the whiB1up-*lacZ* fusion was significantly activated by 8.8±0.2-fold at 24 -hour time point as measured by β-galactosidase activity (Fig. S6F). However, under identical conditions, upon induction of PhoP expression cells carrying whiB1upmut-*lacZ* fusion showed a comparable enzyme activity of 0.95±0.03-fold relative to uninduced cells. Differential expression of the regulator in *M smegmatis* impacting promoter activation was ruled out by comparing induction of PhoP expression in bacterial cells carrying either the WT or the mutant promoter (inset to Fig. S6F). Together, we conclude that presence of the newly identified PhoP-binding site, located immediate upstream of CRP binding site (also see Table 1), is necessary and sufficient for PhoP-dependent activation of *whiB1*.

In binding assays, CRP was unable to bind whiB1up1 to form a complex stable to gel electrophoresis (lanes 2-3, Fig. 6C), and under identical conditions PhoP showed a modest binding to whiB1up1 (lanes 8-9). However, incubation of both PhoP and CRP together (at comparable concentrations) with end-labelled whiB1up1, showed a striking stimulation of ≈5-10-fold of DNA binding leading to the formation of a ‘super-shifted’ band (lanes 4-7). These results suggest that the presence of PhoP significantly stimulates CRP recruitment within the *whiB1* promoter. To determine the composition of the ‘super-shifted’ band (lane 5), the protein components of the complex were extracted as described in the Methods), resolved on a Tricine SDS-PAGE and identified by Western

blotting using anti His antibodies (lane 2, Fig. 6D). Purified regulators were resolved alongside to confirm their relative migration (Fig. 6E). Our results confirm the super-shifted band as a PhoP/CRP/whiB1up1 ternary complex.

To examine the influence of PhoP, we next undertook to investigate *in vivo* recruitment of CRP within the cAMP-inducible promoters of WT-and *ΔphoP*-H37Rv by ChIP. The CRP regulon was previously studied by comparing transcription profiling of WT-H37Rv and a CRP-depleted strain of *M. tuberculosis* H37Rv *(Δcrp*-H37Rv) using RNA-seq and ChIP-seq (37, 51). Formaldehyde-cross-linked DNA-protein complexes of growing *M. tuberculosis* cells were sheared to generate fragments of average size ≈500 bp as described previously (22). In ChIP experiments using anti-CRP antibody, DNA binding was analysed by qPCR (Fig. 6F). Our results show that relative to mock sample, CRP is effectively recruited within its target promoters. For example, *icl1*, and *whiB1*promoters, displayed 5.6±1 and 16.4±2.8-fold enrichments of PCR signals, respectively. In sharp contrast, under identical conditions, *ΔphoP*-H37Rv -derived samples showed insignificant enrichments of CRP within *icl1* (0.7±0.2-fold) and *whiB1* (0.6±0.18-fold), promoters, respectively. However, with identical input DNA sample, we observed a largely comparable CRP recruitment within the CRP-regulated *sucC* promoter (sucCup) (37) in both the WT- and the mutant bacilli. Inset shows a comparable expression of CRP in WT-H37Rv and *ΔphoP*-H37Rv. These results strongly suggest that both mycobacterial regulators are recruited concomitantly within the cAMP-inducible promoters and consistent with PhoP-CRP interaction, absence of PhoP strikingly influences *in vivo* recruitment of CRP.

Discussion

Numerous studies suggest that conditions associated with host environment like low pH, and macrophage interactions often influence mycobacterial cAMP levels (8, 14). Although many bacterial pathogens modulate host cell cAMP levels as a common strategy, the mechanism of mycobacterial cAMP-homeostasis is poorly understood. PhoP, as a master regulator, has been implicated in

controlling diverse mycobacterial stress response. In this study, we sought to investigate whether PhoP is connected to mycobacterial cAMP level. Intriguingly, we find that under normal conditions as well as under carefully controlled single stress conditions, *ΔphoP*-H37Rv shows a significantly lower level of cAMP relative to the WT bacilli (Fig. 1A), and complementation of the mutant restored cAMP level. By comparing cAMP secretion of the WT-H37Rv and the *ΔphoP*-H37Rv, we conclude that altered efficiency of secretion of the mutant does not account for its lower level (Fig. 1B). To examine how PhoP contributes to cAMP homeostasis, we probed regulation of adenylate cyclases and PDEs, which synthesizes and degrades cAMP, respectively (Fig. 1C). Our results unambiguously demonstrate that PhoP functions as a major repressor of Rv0805, encoding cAMP-specific PDE. These results account for a consistently lower level of cytoplasmic cAMP in *ΔphoP*-H37Rv relative to the WT bacilli. It should be noted that Rv0805 is the only cAMP-specific phosphodiesterase identified till date, and is present only in the slow growing pathogenic mycobacteria (15). Thus, the above results showing newly-discovered PhoP-dependent repression of *M. tuberculosis*-specific Rv0805 activity possibly represents the most critical step of mycobacterial cAMP homeostasis.

To examine physiological significance of cAMP homeostasis, we next compared growth of WT-H37Rv, and H37Rv-Rv0805, under specific stress conditions (Fig. 2). Our result showing a significantly higher stress sensitivity of H37Rv-Rv0805, in striking similarity with *ΔphoP*-H37Rv, is consistent with a model suggesting that cAMP homeostasis, at least in part, accounts for mycobacterial stress response. In keeping with this, H37Rv-Rv0805 displays a reduced ability to inhibit phagosome-lysosome fusion similar to *ΔphoP*-H37Rv (Figs. 3A-C). To further investigate how intra-mycobacterial cAMP level impacts on pathogenesis, we show that H37Rv-Rv0805, unlike the WT-H37Rv or H37Rv-Rv0805^{M}, shows a significantly reduced intracellular growth in mice (Figs. 3D-E) as that of *ΔphoP*-H37Rv. Thus, these results are of fundamental significance to establish that PhoP contributes to maintenance of cAMP homeostasis and integrates it to mycobacterial stress response and mechanism of virulence regulation. Together, we identify a novel mycobacterial

pathway as a therapeutic target and provide yet another example of an intimate link between physiology and virulence regulation of the tubercle bacilli.

To investigate the global impact of Rv0805 expression contributing to mycobacterial cAMP homeostasis, we have studied transcriptomic profile of genes by RNA sequencing and compared data from both *ΔphoP*-H37Rv and H37Rv-Rv0805 with WT-H37Rv (Fig. S3). Our results demonstrate that both PhoP-depletion and Rv0805 over-expression significantly impacts expression of a large number of mycobacterial genes [Tables S1, and S2, respectively (Excel spreadsheet)]. Upon a closer inspection, we made two striking observations. First, we noted activation of 21 common genes, and repression of 7 common genes in *ΔphoP*-H37Rv and H37Rv-Rv0805. These observations suggest that PhoP-depletion mimics Rv0805 over-expression in regard to impact on mycobacterial transcriptome. Second, 15 of the 28 genes were found to be part of mycobacterial CRP regulon (37). Together, these results integrate PhoP-dependent Rv0805 expression with functioning of PhoP and CRP as co-activators of cAMP-inducible mycobacterial genes. This observation is in apparent conflict with a previous work by Matange and collaborators (55), suggesting a cAMP-independent transcriptional response in Rv0805 over-expressing *M. tuberculosis* H37Rv. Although both studies were performed with Rv0805 over-expressing bacilli, the fact that important differences in the expression of phosphodiesterases in this study (55) and in our assays – yielding significantly different induction of Rv0805 expression - most likely account for this discrepancy. However, our results showing over-expression of Rv0805 in WT-H37Rv reduces intra-mycobacteria cAMP level (Fig. 2A) is consistent with a previous study correlating Rv0805 expression and intra-mycobacterial cAMP level (7). Further, our experimental data on effect of expression of Rv0805 and $Rv0805^{M}$ on mycobacterial cAMP levels, remarkably correlate with the enzyme activities of the corresponding phosphodiesterases. From these results, we conclude that Rv0805 is a critical regulator of mycobacterial cAMP level.

Having discovered that numerous genes regulated by PhoP and Rv0805 belong to CRP regulon (Fig. S3) and the promoter regions display canonical PhoP and CRP binding sites (Table 1), we sought to explore a functional link between PhoP and CRP. Importantly, presence of PhoP binding sites is consistent with *in vivo* recruitment of PhoP within cAMP-inducible promoters (Fig. 4C). Next, using numerous *in vitro* and *in vivo* approaches, we showed that PhoP interacts with CRP (Fig. 5). While phosphorylation of PhoP was found to be necessary for PhoP-CRP interaction (Fig. 5E), cAMP binding to CRP do not appear to impact PhoP-CRP interaction (Fig. S5G). To examine how a representative promoter recruits both the regulators *in vitro*, we attempted an EMSA experiment using both the purified proteins (Fig. 6C). The fact that PhoP and CRP together form a ternary complex at the *whiB1* promoter, prompted us to investigate a possible inter-dependence of recruitment of the two regulators. Despite effective recruitment of CRP in WT bacilli, CRP recruitment within cAMP-inducible promoters was almost undetectable in *ΔphoP*-H37Rv (Fig. 6F), a result which finds an explanation from PhoP-CRP interaction data (Fig. 5). Given the importance of cAMP inducible gene expression in virulence, PhoP-CRP interactions controlling *in vivo* regulation of genes provides one of the most fundamental biological insights into the mechanism of virulence regulation of *M. tuberculosis*. The finding that PhoP functions as a prerequisite to ensure specific recruitment of CRP within the cAMP inducible promoters, offers a new biological insight into the regulated expression of CRP regulon. Because such a situation might assist PhoP to function efficiently by ensuring CRP binding only to its target promoters already bound to PhoP, it is conceivable that PhoP binding changes DNA conformation, which facilitates CRP recruitment. Therefore, we propose that a DNA-dependent complex interplay of PhoP and CRP via protein-protein interactions most likely controls precise regulation of cAMP inducible genes. Indeed, this model fits well with, explains and integrates previously reported regulations of *icl1* and *whiB1*, independently by PhoP (33, 56) and CRP (37), respectively.

Based on our observations that the N-domains of PhoP and CRP interact to each other (Figs. 6A-B), and effective CRP recruitment is possibly ensured within target promoters already bound to PhoP (Fig. 6F), our model suggests how PhoP-CRP interaction(s) contributes to regulation of cAMP-

inducible genes. These considerations take on more significance in the light of newly-identified PhoP (this study) and previously-identified CRP binding sites (11, 49) within the *whiB1* promoter. The arrangement and spacing between the two binding sites are suggestive of DNA looping, possibly to assist transcription initiation by contributing additional stability to the initiation complex. These results suggest a critically important role of PhoP in binding and transcriptional control of cAMP-inducible genes of H37Rv and establish a molecular mechanism of how these two regulators co-activate expression of these genes in response to phagosomoal stress. However, we do not provide an evidence to suggest 1:1 binding stoichiometry except that as independent regulators, in both cases a dimer of PhoP (57, 58) and CRP (42) bind to target DNA. In *M. tuberculosis*, cAMP-inducible expression of genes including that of an important transcription factor, which remains critical for a successful infection, most likely is under precise regulation as deregulated expression of these genes is likely to alert the immune system to the infection. Given the complex life cycle of the intracellular pathogen which encounters a variety of physiological conditions within the human host, an integration of more than one regulator might be required for *in vivo* functioning to achieve a rather complex regulation of these mycobacterial genes. In fact, reminiscent to our previous study on control mechanism of ESAT-6 secretion (39), this may be possibly a more common strategy than has been previously appreciated.

Materials and Methods

A full explanation of methods studied including bacterial strains and culture conditions, RNA isolation, RNA seq, and ChIP experiments, library construction and high throughput sequencing, RT-qPCR measurements, cloning of numerous PhoP and CRP constructs, expression and purification of proteins, ChIP-qPCR, EMSA, M-PFC assays, cAMP estimation, macrophage infection studies and animal experiments are described in the SI Materials and Methods. The oligonucleotide primer sequences used in cloning are listed in SI Appendix, Table S5; plasmids used in this study are listed in SI Appendix, Table S6; oligonucleotide primer sequences used in RT-qPCR experiments and ChIP-qPCR studies are included in SI Appendix, Table S7, and Table S8, respectively.

Acknowledgements

We thank G. Marcela Rodriguez and Issar Smith (PHRI, New Jersey Medical School - UMDNJ) for Δ*phoP*-H37Rv, and the complemented *M. tuberculosis* H37Rv strains, Adrie Steyn (University of Alabama) for pUAB300/pUAB400 plasmids, and Ashwani Kumar (CSIR-IMTECH) for very helpful discussions. We acknowledge Pragya Priyadarshini for her assistance in docking studies, Neeraj Khatri and members of the animal facility for their help with approval of our projects from the Institutional Animal Ethics Committee, and Sanjeev Khosla for critical reading of the manuscript. Library construction, RNA-sequencing and data analysis have been carried out by Aggrigenome Labs Private Limited (Cochin), India. This study received financial support from intramural grants of CSIR-IMTECH, and by a research grant (to D.S) from SERB (EMR/2016/004904), Department of Science and Technology (DST). H.K., P.P., H.G., R.R.S., B.B., and S.K were supported by CSIR pre-doctoral fellowships.

Author contributions

H.K., P.P., H. G., R.R.S., B.B., and D.S. designed research; H.K., P. P., H.G., R.R.S., B.B., and S. K. performed research; B.S. contributed analytical tools; H.K., P. P., H. G., B.B., B.S. and D.S. analysed data; and D.S. wrote the paper.

Supplemental Data

The supplemental data include six supplemental figures, one supplemental excel spreadsheet which contains data for the heat-map and Venn diagram (Tables S1-S4) showing genes that are differentially regulated either in WT-H37Rv or in indicated strains, and four supplemental tables (Tables S5-S8). Comparisons involve genes annotated in the H37Rv genome and data provided represent average value of two biological repeats. All RNA sequencing data have been deposited in the GEO database with the accession numbers GSE173225. All other relevant data are part of the paper and its supplemental files.

Declaration of interests

The authors declare that they have no conflict of interest.

Figure Legends

Figure 1: PhoP contributes to maintenance of mycobacterial cAMP levels. (A) Intra-mycobacterial cAMP levels were determined by a fluorescence-based assay as described in the Methods, and compared in mycobacterial strains, grown under normal or specific stress conditions. The data represent average values from three biological repeats (*P≤0.05, **P≤0.01). (B) To compare secretion of cAMP by WT-H37Rv and *ΔphoP*-H37Rv, cAMP levels were determined in the corresponding culture filtrates (CF). (C) To investigate regulation of cAMP level, mRNA levels of well-characterized adenylate cyclases, and PDEs were compared in indicated mycobacterial strains by RT-qPCR (**P<0.01) as described in the Methods. The results show average values from biological triplicates, each with two technical repeats (*P≤0.05; **P≤0.01). Nonsignificant difference is not indicated.

Figure 2: cAMP homeostasis and its effect on mycobacterial stress response. (A) To determine the effect of over expression of Rv0805 on intra-mycobacterial cAMP level, WT and mutant Rv0805 proteins ($Rv0805^{M}$, defective for phosphodiesterase activity) were expressed in *M. tuberculosis* H37Rv as described in the Methods. Next, intra-mycobacterial cAMP levels were determined as described in the legend to Fig. 1. It should be noted that similar to *ΔphoP*-H37Rv, H37Rv-Rv0805 (but not H37Rv-$Rv0805^{M}$) showed a considerably lower level of cAMP relative to WT-H37Rv. (B) To compare susceptibility to low pH conditions, indicated mycobacterial strains were grown at pH 4.5. Importantly, similar to *ΔphoP*-H37Rv (filled triangles), H37Rv-Rv0805 (filled diamonds) shows a significant growth defect relative to WT-H37Rv (filled circles). However, H37Rv-Rv0805 (open diamonds) grows comparably well as that of the WT-H37Rv (open circles), under normal pH. (C) Microplate-based assay using Alamar Blue was utilized to examine mycobacterial sensitivity to

increasing concentrations of diamide. In this assay, reduction of Alamar Blue correlates with the change of a non-fluorescent blue to a fluorescent pink appearance, which is directly proportional to bacterial growth. (D) Survival of indicated mycobacterial strains, under normal conditions and in presence of 5 mM diamide, were determined by plotting fluorescence intensity derived from panel C. The data is normalized relative to WT-H37Rv grown in presence of 5 mM diamide. It is noteworthy that both H37Rv-Rv0805 and *ΔphoP*-H37Rv showed comparably higher redox stress sensitivity relative to WT-H37Rv. However, H37Rv-Rv0805^{M} showed a comparable susceptibility to redox stress as that of WT-H37Rv. (E) To compare susceptibility to stress conditions, these mycobacterial strains were next grown in the presence of 50 µM Cumene Hydrogen Peroxide (CHP). Importantly, in presence of CHP, H37Rv-Rv0805 shows a significant growth defect (relative to WT-H37Rv) in striking similarity to *ΔphoP*-H37Rv. The growth experiments were performed as biological duplicates, each with two technical replicates (**P≤0.01; ***P≤0.001).

Figure 3: Mycobacterial cAMP homeostasis and its effect on bacterial survival in macrophages and mice. (A) Murine macrophages were infected with indicated *M. tuberculosis* H37Rv strains. The cells were made visible by LysoTracker; mycobacterial strains were stained with phenolic auramine solution, and the confocal images display merge of two fluorescence signals (Lyso Tracker: red; H37Rv: green; scale bar: 10 µm). (B) Bacterial co-localization of indicated *M. tuberculosis* H37Rv strains. The percentage of auramine labelled strains co-localized with Lysotracker was determined by counting at least 100 infected cells in 10 different fields. The results show the average values with standard deviation determined from three independent experiments (***P≤ 0.001). (C) Pearson's correlation coefficient of images of internalized auramine-labelled mycobacteria and Lysotracker red marker in RAW 264.7 macrophages. Data are representative of mean ± S.D., derived from three independent experiments (*P<0.05; ***P<0.001). (D-E) Survival of mycobacterial strains in mice (D) lung, and (E) spleen after they were given an aerosol infection with ~100 CFU / lung. Mycobacterial load represents mean CFU values with standard deviations obtained from at least five animals per strains used (**P< 0.01; ***P<0.001). (F) Histopathology of lung sections after 4 weeks of infection

with indicated bacterial strains. Sections were stained with hematoxylin and eosin, observed under a light microscope, and images of the pathology sections collected at x40 magnification display granulomas (filled arrows) and alveolar space (empty arrows) (scale bar, 200 µm).

Figure 4: PhoP-depletion or Rv0805 over-expression similarly impact expression of CRP-regulon genes. (A) Quantitative RT-PCR was carried out to compare expression level of cAMP-inducible genes (*icl1*, *umaA* and *whiB1*) in indicated mycobacterial strains, grown under normal and indicated specific stress conditions. The results show average values from biological triplicates, each with two technical repeats (*P≤0.05; **P≤0.01; ***P≤0.001; ****P≤0.0001) as described in the legend to Fig. 1. (B) To examine role of PhoP in *crp* expression, RT-qPCR compared expression levels of *crp* (Rv3676) in WT-H37Rv (empty bar), *ΔphoP*-H37Rv (grey bar) and the complemented mutant (black bar) (***P≤0.001). PhoP-dependent *aprA* expression was shown as a control. (C) *In vivo* recruitment of PhoP within target promoters was examined by ChIP-qPCR (see Methods for further details). *espA* promoter (espAup), and *gapdh* - specific enrichments were used as a positive and negative control, respectively. The experiments were performed in biological duplicates, each with two technical repeats (**P≤0.01; ***P≤0.001), and fold enrichment was determined relative to an IP sample without adding antibody (mock control). Non-significant differences are not indicated.

Figure 5: Probing PhoP-CRP interactions. (A) To investigate PhoP-CRP interaction *in vitro*, crude extract expressing His_6-tagged CRP was incubated with glutathione sepharose previously immobilized with GST-PhoP. Bound proteins (lane 1) were analyzed by Western blot using anti-His (upper panel) or anti-GST antibody (lower panel). Lane 1 shows presence of CRP bound to GST-PhoP. Identical experiment used glutathione Sepharose immobilized with GST alone (lane 2), or the resin alone (lane 3); lane 4 resolved recombinant His_6-tagged CRP. (B-C) To probe protein-protein interaction by mycobacterial protein fragment complementation (M-PFC) assays, *M. smegmatis* expressing either *M. tuberculosis* (B) PhoP and CRP or (C) PhoP and CMR, were grown on

7H10/hyg/kan plates in presence of TRIM, and growth was examined for strains co-expressing indicated fusion constructs. In both cases, empty vectors were included as negative controls, and co-expression of pUAB400-*phoP*/pUAB300-*phoR* (as a positive control) encoding PhoP and PhoR, respectively, showed *M. smegmatis* growth in presence of TRIM. All the strains grew well in absence of TRIM. (D) To verify expression of *M. tuberculosis* CRP and CMR in *M. smegmatis*, mRNA levels of the regulators were compared by RT-qPCR. Average fold changes in mRNA levels from two biological repeats (each with two technical repeats) are plotted, and non-significant difference is not indicated. (E) Next, PhoP-CRP interaction was probed by M-PFC experiments using *M. smegmatis* strain co-expressing PhoPD71N (phosphorylation defective point mutant of PhoP) and CRP, respectively. Strains co-expressing indicated fusions constructs, and appropriate negative and positive controls were as described in panel B. (F) To examine PhoP-CRP interaction *in vivo*, crude cell lysates of *ΔphoP*-H37Rv expressing His_6-tagged PhoP (p19kpro-*phoP*; Table S6) was incubated with pre-equilibrated Ni-NTA and eluted with 250 mM imidazole; lane 1, input sample; lane 2, control elution from the crude lysate of cells lacking *phoP* expression; lane 3, co-elution of CRP with PhoP. Blots were probed with anti-PhoP and anti-CRP antibody.

Figure 6: PhoP promotes CRP recruitment and regulates cAMP- inducible gene expression. (A-B) PhoP-CRP interaction was probed by *in vitro* pull-down assays using either (A) His-tagged CRP and GST-tagged PhoP domains (GST-PhoPN and GST-PhoPC, respectively) or (B) GST-tagged PhoP and His-tagged CRP domains (His-CRPN, and His-CRPC, respectively). The domain constructs are listed in Table S6. Fractions of bound proteins were analysed by Western blot using anti-His (upper panel) or anti-GST antibody (lower panel). Control sets include glutathione Sepharose immobilized with GST (lane 3), or the resin (lane 4) alone; lane 5 of panel A resolved purified CRP, while lanes 5, and 6 of panel B resolved purified CRPN, and CRPC, respectively. (C) To examine effect of PhoP-CRP interaction in presence of the cognate promoter DNA, EMSA experiments compared end-labelled whiB1up1 binding to increasing concentrations of purified CRP (lanes 2-3), PhoP (lanes 8-9), and both PhoP and CRP together (lanes 4-7). The assay conditions, sample analyses, and detection are

described in the Methods section. (D) Western blot analyses of protein fraction extracted from the excised gel fragment representing the complex (lane 5), as indicated by a box, was probed by anti-His antibody in lane 2; lane 1 resolved purified PhoP. (E) Tricine SDS-PAGE electrophoretic analysis of recombinant His-tagged CRP (lane 1) and PhoP (lane 2); lane 3 resolved marker proteins of indicated molecular masses. Protein samples were visualized by Coomassie blue staining. (F) Fold PCR enrichment due to CRP binding to indicated cAMP-inducible promoters was investigated by ChIP-qPCR as described in the Methods, and data were compared between the WT-H37Rv and *ΔphoP*-H37Rv (**$P \leq 0.01$). Inset compares CRP expression in ≈10 μg of indicated crude cell-lysates as probed by anti-CRP antibody; identical extracts were probed with anti-RpoB antibody as a loading control.

Figure 7: Schematic model depicts the molecular events determining mycobacterial cAMP homeostasis and cAMP-inducible gene expression. While specific stress conditions elevate level of intra-mycobacterial cAMP, degradation of it is controlled by cAMP-specific PDE Rv0805, which is regulated by the mycobacterial *phoP* locus. Thus, cAMP homeostasis is a key event during intracellular survival of *M. tuberculosis*, as CRP controls expression of cAMP inducible genes with the assistance of the master regulator PhoP via protein-protein interactions. Together, these molecular events regulate intra-mycobacterial cAMP level, mitigate stress by controlling expression of cAMP-inducible genes and contribute to survival of the bacilli in cellular and animal models.

Table 1

Localizing PhoP and CRP binding sites within selected promoters of CRP regulon*

Rv number	Gene name	PhoP binding Site	PhoP coordinates	CRP binding site	CRP coordinates	Annotated function
Rv0079	*Rv0079*	CCTCAGCTTCTGCGCAGC	-215 to -232	GGTGACACAGCCCACA	-95 to -110	unknown
Rv0467**	*icl1*	CGACCGCGCTGTTACAAC	-333 to -350	TGTTACAACGCTCACA	-49 to -64	involved in glyoxylate bypass
Rv0469**	*uma A*	GCAAGGCGAGATCACAGA	-88 to -105	TGTGACAGCCGTTGCG	-326 to -341	involved in mycolic acid modification or synthesis
Rv0572c	*Rv0572c*	TCCCGGCTTGACCGCGGC	-127 to -144	GGTGAATGCCCGCACC	-77 to -92	unknown
Rv1057	*Rv1057*	GCACAGCACGGTTGCTGT	-103 to -120	CGTGACCTAGGTAACA	-233 to -248	unknown
Rv1736c	*narX*	TCGCCGCGGCGTTGCAGC	-308 to -325	GGTCGGCTCGGTCACC	-183 to -198	nitrate reduction and in the persistence in the host
Rv1997	*ctpF*	TCGCTCCACGCGTGCAGC	-532 to -549	GATGTCGTCGTGCACA	-399 to -414	metal cation-transporting ATPase
Rv2005c	*Rv2005c*	TGACGACGATGCCACAGC	-123 to -140	TGTGCCCGTAGTTACG	-569 to -584	unknown
Rv2007c	*fdxA*	TCCCAGCTCGCGCCGAGC	-505 to -522	AGTGACGAACTTGACG	-79 to -94	involved in electron transfer
Rv2624c	*Rv2624c*	GCGCTGCCGCTGCACAGC	-237 to -254	GCTGACCGCGCTCCTA	-195 to -210	unknown
Rv2626c	*hrp1*	ACGCGCCACGGACACAGC	-531 to -548	TGTGACGGATGTGGCA	-401 to -416	unknown
Rv2029c	*pfkB*	GAACGGCAAAGTCACTAC	-149 to -166	GGTGACGAGTCGCGCA	-394 to -409	glycolysis: converts sugar-1-P to sugar-1,6-P
Rv2030c	*Rv2030c*	TCCCCGAGTTTTCTGAGC	-386 to -403	TGTCACCCGGCGCTCG	+24 to +39	unknown
Rv2031c	*hspX*	GCACCGTCGCTCCACAAC	-257 to -274	GGGGACTTCTGTCCCT	-65 to -80	stress protein induced by anoxia
Rv2032	*acg*	TCCCCGAGTTTTCTGAGC	-239 to -256	AGGGACAGAAGTCCCC	-117 to -132	unknown
Rv2987c	*leuD*	ACCTTGCGGCCACGCAGC	-326 to -343	TGTCACCTGGGGCACC	-550 to -565	involved in leucine biosynthesis
Rv3219**	*whiB1*	ACTGGGTAAGGGCTGTGG	-191 to -208	AGTGAGATAGCCCACG	-161 to -176	involved in transcriptional mechanism
Rv3824c	*papA1*	GGAAAGCAACTACACGGC	-511 to -528	TGGGACCCAGCGCCCG	+40 to +55	involved in sulfolipid-1 (SL-1) biosynthesis

*RNA-sequencing analyses uncover 15 genes which belong to CRP regulon and are commonly regulated either by depletion of PhoP or by over-expression of Rv0805.

** 3 more genes were identified to be commonly regulated by PhoP and CRP based on the corresponding transcriptomic data (31, 37) .

Both PhoP and CRP binding sites were identified in selected *M. tuberculosis* H37Rv promoters by scanning for respective ChIP-seq derived consensus sequence motifs (31, 37) using MEME Suite software (59). Only motifs of nucleotide sequences with a corresponding p-value of 0.01 or less were considered. RNA-seq analyses were carried out as described in the Methods using two biological repeats and results shown are average of two independent measurements. Nucleotide sequences of indicated binding sites are numbered with respect to the corresponding ORF start sites.

References

1. J. D. Ernst, The immunological life cycle of tuberculosis. *Nat Rev Immunol* **12**, 581-591 (2012).
2. D. G. Russell, Mycobacterium tuberculosis and the intimate discourse of a chronic infection. *Immunol Rev* **240**, 252-268 (2011).
3. K. H. Rohde, R. B. Abramovitch, D. G. Russell, Mycobacterium tuberculosis invasion of macrophages: linking bacterial gene expression to environmental cues. *Cell Host Microbe* **2**, 352-364 (2007).
4. K. A. McDonough, A. Rodriguez, The myriad roles of cyclic AMP in microbial pathogens: from signal to sword. *Nat Rev Microbiol* **10**, 27-38 (2011).
5. T. Klengel *et al.*, Fungal adenylyl cyclase integrates CO2 sensing with cAMP signaling and virulence. *Curr Biol* **15**, 2021-2026 (2005).
6. L. Mallet, G. Renault, M. Jacquet, Functional cloning of the adenylate cyclase gene of Candida albicans in Saccharomyces cerevisiae within a genomic fragment containing five other genes, including homologues of CHS6 and SAP185. *Yeast* **16**, 959-966 (2000).
7. N. Agarwal, G. Lamichhane, R. Gupta, S. Nolan, W. R. Bishai, Cyclic AMP intoxication of macrophages by a Mycobacterium tuberculosis adenylate cyclase. *Nature* **460**, 98-102 (2009).
8. G. Bai, D. D. Schaak, K. A. McDonough, cAMP levels within Mycobacterium tuberculosis and Mycobacterium bovis BCG increase upon infection of macrophages. *FEMS Immunol Med Microbiol* **55**, 68-73 (2009).
9. D. B. Lowrie, P. S. Jackett, N. A. Ratcliffe, Mycobacterium microti may protect itself from intracellular destruction by releasing cyclic AMP into phagosomes. *Nature* **254**, 600-602 (1975).
10. M. A. Gazdik, K. A. McDonough, Identification of cyclic AMP-regulated genes in Mycobacterium tuberculosis complex bacteria under low-oxygen conditions. *J Bacteriol* **187**, 2681-2692 (2005).
11. N. Agarwal, T. R. Raghunand, W. R. Bishai, Regulation of the expression of whiB1 in Mycobacterium tuberculosis: role of cAMP receptor protein. *Microbiology* **152**, 2749-2756 (2006).
12. G. Bai, L. A. McCue, K. A. McDonough, Characterization of Mycobacterium tuberculosis Rv3676 (CRPMt), a cyclic AMP receptor protein-like DNA binding protein. *J Bacteriol* **187**, 7795-7804 (2005).
13. L. Rickman *et al.*, A member of the cAMP receptor protein family of transcription regulators in Mycobacterium tuberculosis is required for virulence in mice and controls transcription of the rpfA gene coding for a resuscitation promoting factor. *Mol Microbiol* **56**, 1274-1286 (2005).
14. M. A. Gazdik, G. Bai, Y. Wu, K. A. McDonough, Rv1675c (cmr) regulates intramacrophage and cyclic AMP-induced gene expression in Mycobacterium tuberculosis-complex mycobacteria. *Mol Microbiol* **71**, 434-448 (2009).
15. G. S. Knapp, K. A. McDonough, Cyclic AMP Signaling in Mycobacteria. *Microbiol Spectr* **2** (2014).
16. C. Nathan, M. U. Shiloh, Reactive oxygen and nitrogen intermediates in the relationship between mammalian hosts and microbial pathogens. *Proc Natl Acad Sci U S A* **97**, 8841-8848 (2000).
17. T. R. Rustad, A. M. Sherrid, K. J. Minch, D. R. Sherman, Hypoxia: a window into Mycobacterium tuberculosis latency. *Cell Microbiol* **11**, 1151-1159 (2009).
18. L. G. Wayne, C. D. Sohaskey, Nonreplicating persistence of mycobacterium tuberculosis. *Annu Rev Microbiol* **55**, 139-163 (2001).

792 19. R. B. Abramovitch, K. H. Rohde, F. F. Hsu, D. G. Russell, aprABC: a Mycobacterium
793 tuberculosis complex-specific locus that modulates pH-driven adaptation to the macrophage
794 phagosome. *Mol Microbiol* **80**, 678-694 (2011).
795 20. R. Bansal, V. Anil Kumar, R. R. Sevalkar, P. R. Singh, D. Sarkar, Mycobacterium tuberculosis
796 virulence-regulator PhoP interacts with alternative sigma factor SigE during acid-stress
797 response. *Mol Microbiol* **104**, 400-411 (2017).
798 21. S. Tan, N. Sukumar, R. B. Abramovitch, T. Parish, D. G. Russell, Mycobacterium tuberculosis
799 responds to chloride and pH as synergistic cues to the immune status of its host cell. *PLoS*
800 *Pathog* **9**, e1003282 (2013).
801 22. R. Singh, V. Anil Kumar, A. K. Das, R. Bansal, D. Sarkar, A transcriptional co-repressor
802 regulatory circuit controlling the heat-shock response of Mycobacterium tuberculosis. *Mol*
803 *Microbiol* **94**, 450-465 (2014).
804 23. R. R. Sevalkar *et al.*, Functioning of Mycobacterial Heat Shock Repressors Requires the
805 Master Virulence Regulator PhoP. *J Bacteriol* **201** (2019).
806 24. J. J. Baker, B. K. Johnson, R. B. Abramovitch, Slow growth of Mycobacterium tuberculosis at
807 acidic pH is regulated by phoPR and host-associated carbon sources. *Mol Microbiol* **94**, 56-69
808 (2014).
809 25. B. K. Dass, R. Sharma, A. R. Shenoy, R. Mattoo, S. S. Visweswariah, Cyclic AMP in
810 mycobacteria: characterization and functional role of the Rv1647 ortholog in Mycobacterium
811 smegmatis. *J Bacteriol* **190**, 3824-3834 (2008).
812 26. D. Dittrich, C. Keller, S. Ehlers, J. E. Schultz, P. Sander, Characterization of a Mycobacterium
813 tuberculosis mutant deficient in pH-sensing adenylate cyclase Rv1264. *Int J Med Microbiol*
814 **296**, 563-566 (2006).
815 27. A. Zaveri *et al.*, Mycobacterial STAND adenylyl cyclases: The HTH domain binds DNA to form
816 biocrystallized nucleoids. *Biophys J* **120**, 1231-1246 (2021).
817 28. A. R. Shenoy, N. Sreenath, M. Podobnik, M. Kovacevic, S. S. Visweswariah, The Rv0805 gene
818 from Mycobacterium tuberculosis encodes a 3',5'-cyclic nucleotide phosphodiesterase:
819 biochemical and mutational analysis. *Biochemistry* **44**, 15695-15704 (2005).
820 29. A. R. Shenoy *et al.*, Structural and biochemical analysis of the Rv0805 cyclic nucleotide
821 phosphodiesterase from Mycobacterium tuberculosis. *J Mol Biol* **365**, 211-225 (2007).
822 30. M. Podobnik *et al.*, A mycobacterial cyclic AMP phosphodiesterase that moonlights as a
823 modifier of cell wall permeability. *J Biol Chem* **284**, 32846-32857 (2009).
824 31. L. Solans *et al.*, The PhoP-dependent ncRNA Mcr7 modulates the TAT secretion system in
825 Mycobacterium tuberculosis. *PLoS Pathog* **10**, e1004183 (2014).
826 32. A. Parikh *et al.*, Development of a new generation of vectors for gene expression, gene
827 replacement, and protein-protein interaction studies in mycobacteria. *Appl Environ*
828 *Microbiol* **79**, 1718-1729 (2013).
829 33. S. B. Walters *et al.*, The Mycobacterium tuberculosis PhoPR two-component system
830 regulates genes essential for virulence and complex lipid biosynthesis. *Mol Microbiol* **60**,
831 312-330 (2006).
832 34. R. Goyal *et al.*, Phosphorylation of PhoP protein plays direct regulatory role in lipid
833 biosynthesis of Mycobacterium tuberculosis. *J Biol Chem* **286**, 45197-45208 (2011).
834 35. W. Frigui *et al.*, Control of M. tuberculosis ESAT-6 secretion and specific T cell recognition by
835 PhoP. *PLoS Pathog* **4**, e33 (2008).
836 36. A. Romagnoli *et al.*, ESX-1 dependent impairment of autophagic flux by Mycobacterium
837 tuberculosis in human dendritic cells. *Autophagy* **8**, 1357-1370 (2012).
838 37. C. Kahramanoglou *et al.*, Genomic mapping of cAMP receptor protein (CRP Mt) in
839 Mycobacterium tuberculosis: relation to transcriptional start sites and the role of CRPMt as a
840 transcription factor. *Nucleic Acids Res* **42**, 8320-8329 (2014).

841 38. K. A. De Smet, K. E. Kempsell, A. Gallagher, K. Duncan, D. B. Young, Alteration of a single
842 amino acid residue reverses fosfomycin resistance of recombinant MurA from
843 Mycobacterium tuberculosis. *Microbiology* **145 (Pt 11)**, 3177-3184 (1999).
844 39. V. Anil Kumar *et al.*, EspR-dependent ESAT-6 Protein Secretion of Mycobacterium
845 tuberculosis Requires the Presence of Virulence Regulator PhoP. *J Biol Chem* **291**, 19018-
846 19030 (2016).
847 40. A. Singh, D. Mai, A. Kumar, A. J. Steyn, Dissecting virulence pathways of Mycobacterium
848 tuberculosis through protein-protein association. *Proc Natl Acad Sci U S A* **103**, 11346-11351
849 (2006).
850 41. R. Chen, L. Li, Z. Weng, ZDOCK: an initial-stage protein-docking algorithm. *Proteins* **52**, 80-87
851 (2003).
852 42. M. C. Reddy *et al.*, Structural insights into the mechanism of the allosteric transitions of
853 Mycobacterium tuberculosis cAMP receptor protein. *J Biol Chem* **284**, 36581-36591 (2009).
854 43. M. A. Marti-Renom *et al.*, Comparative protein structure modeling of genes and genomes.
855 *Annu Rev Biophys Biomol Struct* **29**, 291-325 (2000).
856 44. B. Webb, A. Sali, Comparative Protein Structure Modeling Using MODELLER. *Curr Protoc*
857 *Bioinformatics* **47**, 5 6 1-32 (2014).
858 45. B. Pierce, Z. Weng, ZRANK: reranking protein docking predictions with an optimized energy
859 function. *Proteins* **67**, 1078-1086 (2007).
860 46. E. Krissinel, K. Henrick, Inference of macromolecular assemblies from crystalline state. *J Mol*
861 *Biol* **372**, 774-797 (2007).
862 47. A. Pathak, R. Goyal, A. Sinha, D. Sarkar, Domain structure of virulence-associated response
863 regulator PhoP of Mycobacterium tuberculosis: role of the linker region in regulator-
864 promoter interaction(s). *J Biol Chem* **285**, 34309-34318 (2010).
865 48. D. T. Gallagher, N. Smith, S. K. Kim, H. Robinson, P. T. Reddy, Profound asymmetry in the
866 structure of the cAMP-free cAMP Receptor Protein (CRP) from Mycobacterium tuberculosis.
867 *J Biol Chem* **284**, 8228-8232 (2009).
868 49. M. Stapleton *et al.*, Mycobacterium tuberculosis cAMP receptor protein (Rv3676) differs
869 from the Escherichia coli paradigm in its cAMP binding and DNA binding properties and
870 transcription activation properties. *J Biol Chem* **285**, 7016-7027 (2010).
871 50. J. Green *et al.*, Cyclic-AMP and bacterial cyclic-AMP receptor proteins revisited: adaptation
872 for different ecological niches. *Curr Opin Microbiol* **18**, 1-7 (2014).
873 51. L. Rickman *et al.*, A member of the cAMP receptor protein family of transcription regulators
874 in Mycobacterium tuberculosis is required for virulence in mice and controls transcription of
875 the rpfA gene coding for a resuscitation promoting factor. *Mol Microbiol* **56**, 1274-1286
876 (2005).
877 52. X. He, S. Wang, DNA consensus sequence motif for binding response regulator PhoP, a
878 virulence regulator of Mycobacterium tuberculosis. *Biochemistry* **53**, 8008-8020 (2014).
879 53. O. Dussurget *et al.*, Transcriptional control of the iron-responsive fxbA gene by the
880 mycobacterial regulator IdeR. *J Bacteriol* **181**, 3402-3408 (1999).
881 54. S. Ehrt *et al.*, Controlling gene expression in mycobacteria with anhydrotetracycline and Tet
882 repressor. *Nucleic Acids Res* **33**, e21 (2005).
883 55. N. Matange, D. M. Hunt, R. S. Buxton, S. S. Visweswariah, Overexpression of the Rv0805
884 phosphodiesterase elicits a cAMP-independent transcriptional response. *Tuberculosis*
885 *(Edinb)* **93**, 492-500 (2013).
886 56. J. Gonzalo-Asensio *et al.*, PhoP: a missing piece in the intricate puzzle of Mycobacterium
887 tuberculosis virulence. *PLoS One* **3**, e3496 (2008).
888 57. S. Gupta, A. Pathak, A. Sinha, D. Sarkar, Mycobacterium tuberculosis PhoP recognizes two
889 adjacent direct-repeat sequences to form head-to-head dimers. *J Bacteriol* **191**, 7466-7476
890 (2009).

58. S. Menon, S. Wang, Structure of the response regulator PhoP from Mycobacterium tuberculosis reveals a dimer through the receiver domain. *Biochemistry* **50**, 5948-5957 (2011).
59. C. E. Grant, T. L. Bailey, W. S. Noble, FIMO: scanning for occurrences of a given motif. *Bioinformatics* **27**, 1017-1018 (2011).

Figure 1

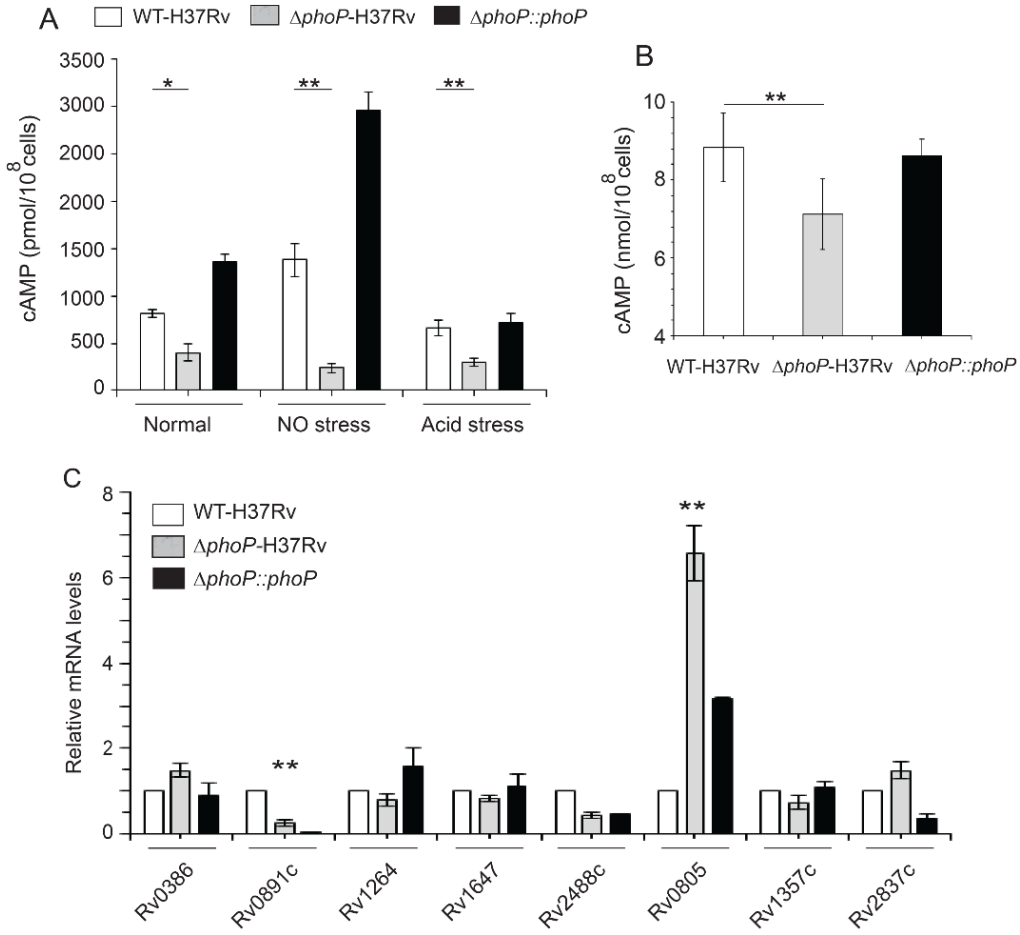
A
WT-H37Rv
ΔphoP-H37Rv
ΔphoP::phoP
cAMP (pmol/10^8 cells)
3500
3000
2000
2000
1500
1000
500
0
*
**
**
Normal
NO stress
Acid stress
B
cAMP (nmol/10^8 cells)
10
8
6
4
**
WT-H37Rv
ΔphoP-H37Rv
ΔphoP::phoP
C
Relative mRNA levels
8
6
4
2
0
WT-H37Rv
ΔphoP-H37Rv
ΔphoP::phoP
**
**
Rv0386
Rv0891c
Rv1264
Rv1647
Rv2488c
Rv0805
Rv1357c
Rv2837c

Figure 2

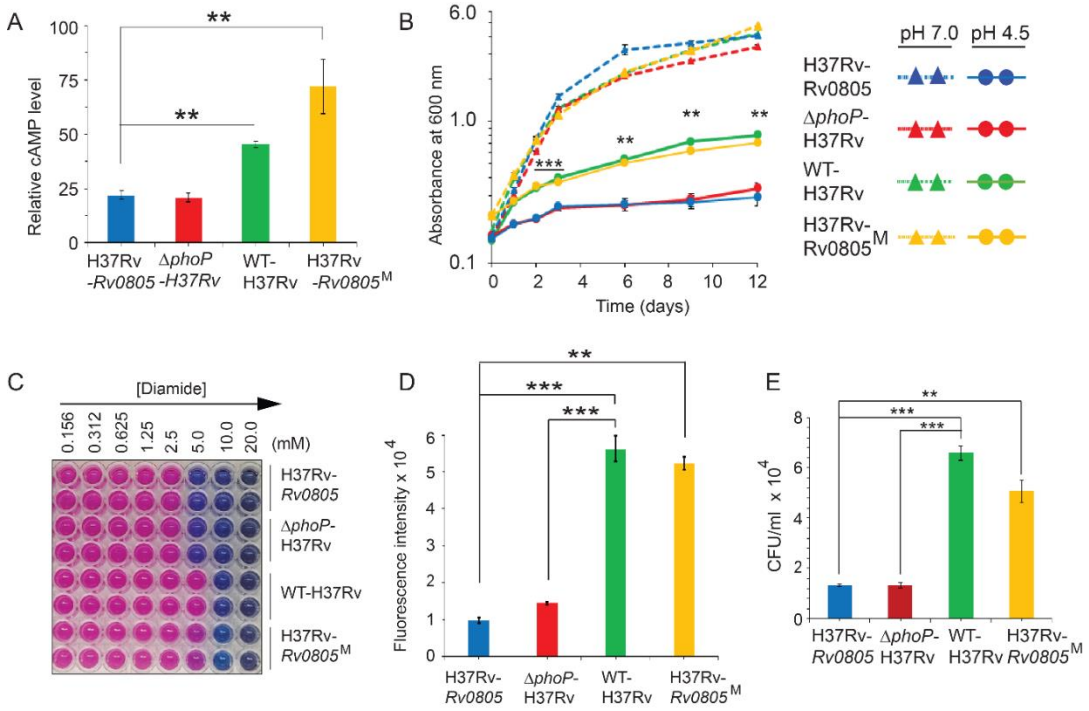
A
Relative cAMP level
100
75
50
25
0
**
**
H37Rv -Rv0805
ΔphoP -H37Rv
WT-H37Rv
H37Rv -Rv0805M
B
Absorbance at 600 nm
6.0
1.0
0.1
0
2
4
6
8
10
12
Time (days)
***
**
**
**
pH 7.0
pH 4.5
H37Rv-Rv0805
ΔphoP-H37Rv
WT-H37Rv
H37Rv-Rv0805M
C
[Diamide]
0.156
0.312
0.625
1.25
2.5
5.0
10.0
20.0
(mM)
H37Rv-Rv0805
ΔphoP-H37Rv
WT-H37Rv
H37Rv-Rv0805M
D
Fluorescence intensity x 10^4
6
5
4
3
2
1
0
**
***
***
H37Rv-Rv0805
ΔphoP-H37Rv
WT-H37Rv
H37Rv-Rv0805M
E
CFU/ml x 10^4
8
6
4
2
0
**
***
***
H37Rv-Rv0805
ΔphoP-H37Rv
WT-H37Rv
H37Rv-Rv0805M

Figure 3

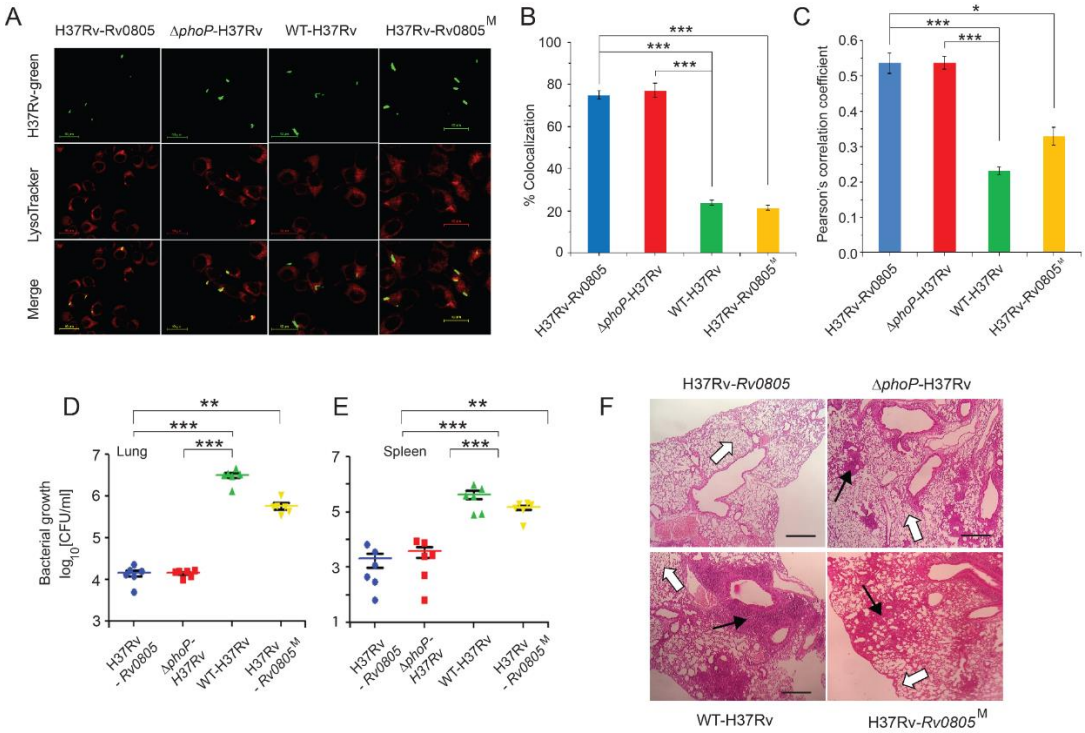
A
H37Rv-Rv0805
ΔphoP-H37Rv
WT-H37Rv
H37Rv-Rv0805M
H37Rv-green
LysoTracker
Merge
B
% Colocalization
H37Rv-Rv0805
ΔphoP-H37Rv
WT-H37Rv
H37Rv-Rv0805M
C
Pearson's correlation coefficient
D
Lung
Bacterial growth log10[CFU/ml]
E
Spleen
F
H37Rv-Rv0805
ΔphoP-H37Rv
WT-H37Rv
H37Rv-Rv0805M

Figure 4

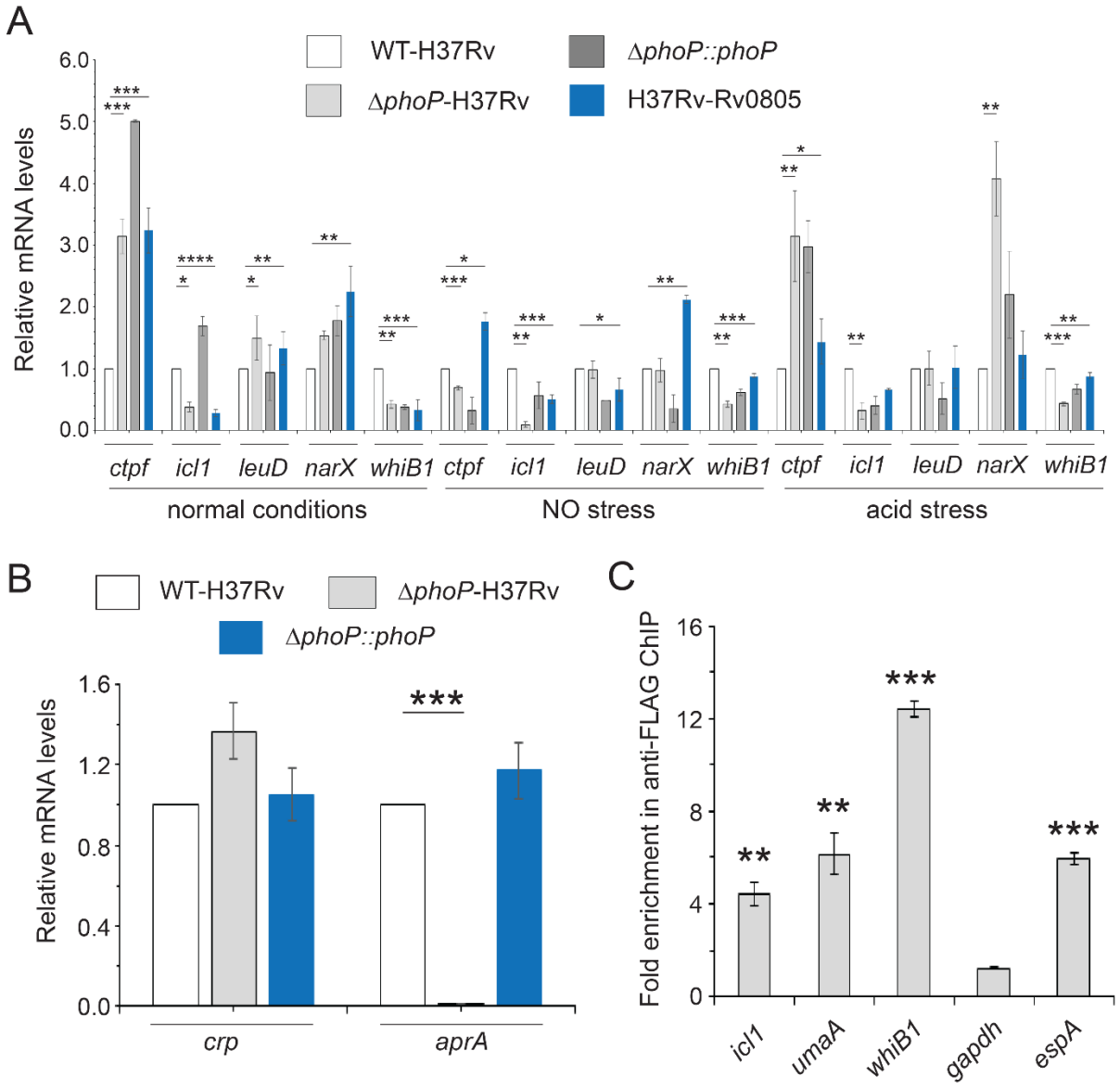
A
WT-H37Rv
ΔphoP-H37Rv
ΔphoP::phoP
H37Rv-Rv0805
Relative mRNA levels
6.0
5.0
4.0
3.0
2.0
1.0
0.0
ctpf icl1 leuD narX whiB1 ctpf icl1 leuD narX whiB1 ctpf icl1 leuD narX whiB1
normal conditions
NO stress
acid stress
B
WT-H37Rv
ΔphoP-H37Rv
ΔphoP::phoP
Relative mRNA levels
1.6
1.2
0.8
0.4
0.0
crp
aprA
C
Fold enrichment in anti-FLAG ChIP
16
12
8
4
0
icl1
umaA
whiB1
gapdh
espA

Figure 5

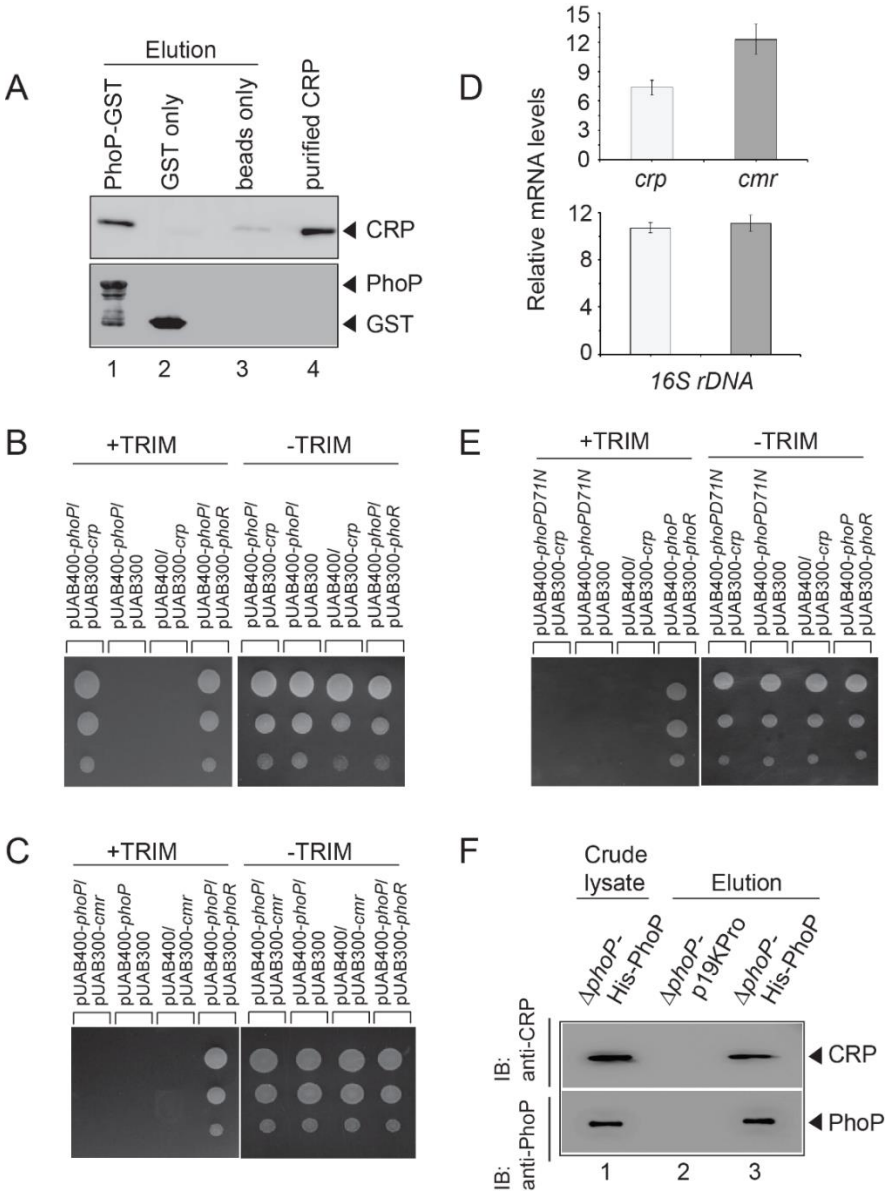
A
Elution
PhoP-GST
GST only
beads only
purified CRP
CRP
PhoP
GST
1 2 3 4
D
Relative mRNA levels
crp
cmr
16S rDNA
B
+TRIM
-TRIM
pUAB400-phoPI pUAB300-crp
pUAB400-phoPI pUAB300
pUAB400/ pUAB300-crp
pUAB400-phoPI pUAB300-phoR
E
pUAB400-phoPD71N pUAB300-crp
pUAB400-phoPD71N pUAB300
pUAB400/ pUAB300-crp
pUAB400-phoP pUAB300-phoR
C
pUAB400-phoPI pUAB300-cmr
pUAB400-phoP pUAB300
pUAB400/ pUAB300-cmr
F
Crude lysate
Elution
ΔphoP-His-PhoP
ΔphoP-p19KPro
IB: anti-CRP
IB: anti-PhoP
1 2 3

Figure 6

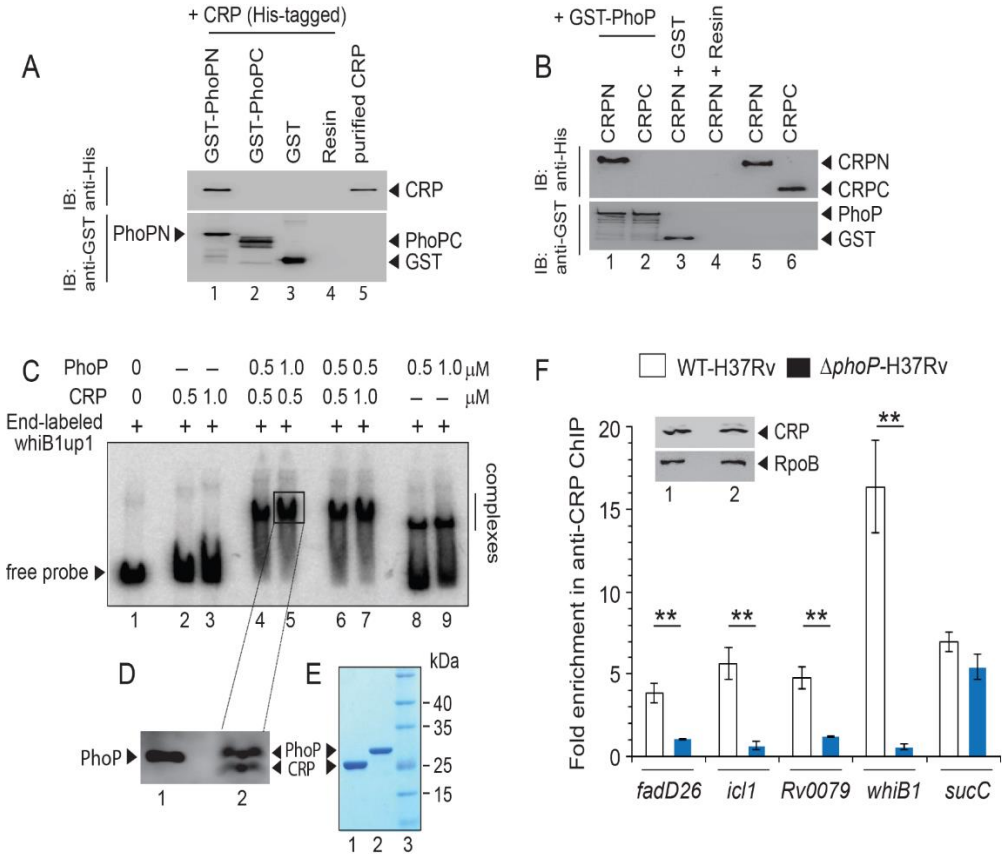
A
+ CRP (His-tagged)
GST-PhoPN
GST-PhoPC
GST
Resin
purified CRP
IB: anti-His
IB: anti-GST
CRP
PhoPN
PhoPC
GST
1 2 3 4 5
B
+ GST-PhoP
CRPN
CRPC
CRPN + GST
CRPN + Resin
CRPN
CRPC
IB: anti-His
IB: anti-GST
CRPN
CRPC
PhoP
GST
1 2 3 4 5 6
C
PhoP 0 – – 0.5 1.0 0.5 0.5 0.5 1.0 μM
CRP 0 0.5 1.0 0.5 0.5 0.5 1.0 – – μM
End-labeled whiB1up1
free probe
complexes
1 2 3 4 5 6 7 8 9
D
PhoP
1 2
E
kDa
40
35
25
15
PhoP
CRP
1 2 3
F
WT-H37Rv
ΔphoP-H37Rv
Fold enrichment in anti-CRP ChIP
20
15
10
5
0
CRP
RpoB
1 2
**
fadD26
icl1
Rv0079
whiB1
sucC

Figure 7

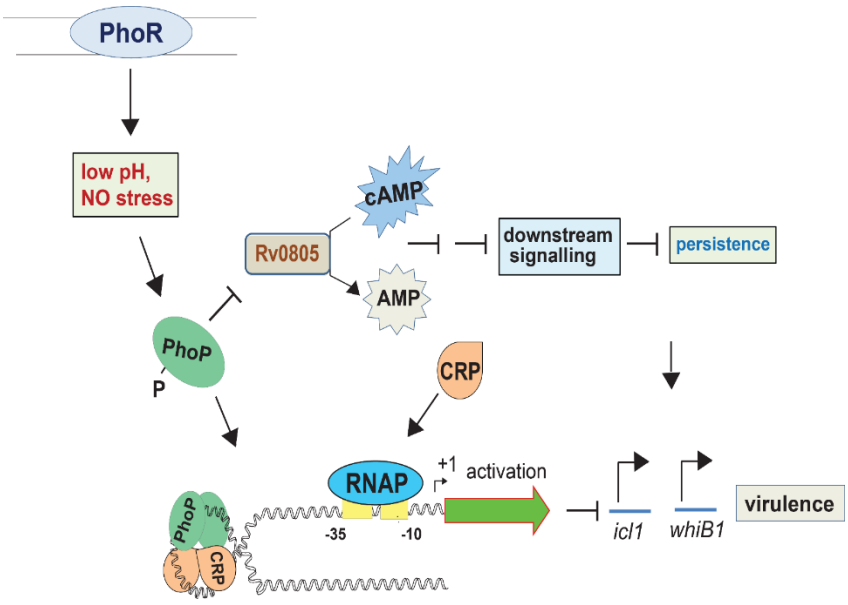
PhoR
low pH,
NO stress
cAMP
Rv0805
AMP
downstream
signalling
persistence
PhoP
P
CRP
RNAP
+1
activation
PhoP
CRP
-35
-10
icl1
whiB1
virulence